Modeling of High-k-Metal-Gate-Stacks Using the Non-Equilibrium Green's Function Formalism

O. Baumgartner, M. Karner, and H. Kosina

Institute for Microelectronics, TU Wien
Gußhausstraße 27–29, A–1040 Wien, Austria
E-mail: {baumgartner|karner|kosina}@iue.tuwien.ac.at

***Abstract*—A high-k-Metal-Gate stack has been investigated using an open boundary model based on the non-equilibrium Green's function formalism. The numerical energy integration, which is crucial because of the very narrow resonant states, is pointed out in detail. The model has been benchmarked against the established classical and closed boundary Schrödinger-Poisson model. In contrast to the established models, the solution covers distinct resonant states with a realistic broadening and results in a major difference in the current density spectrum.**

I. Introduction

The recent introduction of high-k-metal-gate transistors [1] draws the attention to a more accurate modeling of gate leakage current. Two different models are commonly used, namely the Tsu-Esaki formula [2] and the quasi-bound state (QBS) tunneling formalism [3]. The current expressions are given by

$$J_{\mathrm{Tsu}} = N_{\mathrm{Tsu}} \int TC(\mathcal{E}) SF(\mathcal{E})\, \mathrm{d}\mathcal{E} \tag{1}$$

according to Tsu and Esaki, and

$$J_{\mathrm{QBS}} = N_{\mathrm{QBS}} \sum_i \frac{n_i}{\tau_i} \tag{2}$$

for the QBS case. Expression (1) relies on a the transmission coefficient TC of the barrier and a supply function SF, determined by the carrier distributions in the gate and channel regions. The QBS method is based on the electron populations n_i of the discrete subbands in the MOS inversion layer and a finite lifetime τ_i. Both approaches neglect the carrier density in the dielectric due to the hard wall boundary conditions assumed and are thus inconsistent with the non-vanishing current density.

II. Non-Equilibrium Green's Functions

A more rigorous description by the non-equilibrium Green's functions (NEGF) formalism [4] overcomes the aforementioned problem. It allows for a full quantum mechanical treatment and yields the current density consistently with the carrier density. The influence of level broadening due to scattering processes was modeled by means of an optical potential [5]. Using this model a high-k gate-stack has been analyzed.

The gate and the bulk regions have been assumed to be in thermal equilibrium and are characterized by the Fermi energies $\mathcal{E}_{\mathrm{FG}}$ and $\mathcal{E}_{\mathrm{FB}}$, respectively (c.f. Fig.1). The leakage current through the gate dielectric, which separates the equilibrium regions, has been calculated assuming ballistic transport between the two reservoirs [6], [7]. The retarded and advanced Green's functions are determined by

$$\begin{aligned} G^{\mathrm{R}}(\mathbf{r},\mathbf{r}',\mathcal{E}) &= G^{\mathrm{A}\dagger}(\mathbf{r},\mathbf{r}',\mathcal{E}) \\ &= [\mathcal{E}I - H(\mathbf{r},\mathbf{r}',\mathcal{E}) - \Sigma^{\mathrm{R}}(\mathbf{r},\mathbf{r}',\mathcal{E})]^{-1}, \end{aligned} \tag{3}$$

where $H(\mathbf{r},\mathbf{r}',\mathcal{E})$ is the Hamiltonian of the system and $\Sigma^{\mathrm{R}}(\mathbf{r},\mathbf{r}',\mathcal{E})$ is the retarded self-energy. The optical potential determined by the carrier lifetime τ is added to the diagonal elements of the Hamiltonian:

$$H(\mathbf{r},\mathbf{r},\mathcal{E}) = H_0(\mathbf{r},\mathbf{r},\mathcal{E}) + \mathrm{i}\hbar/(2\tau). \tag{4}$$

Assuming Fermi Dirac statistics, the occupation is given by $f_{\mathrm{G,B}}(\mathcal{E}) = N_{\mathrm{C,2D}}\mathcal{F}_0\left(\beta\left(\mathcal{E}_{\mathrm{F_{G,B}}} - \mathcal{E}\right)\right)$ with $\beta = 1/\mathrm{k_B}T$. Within the equilibrium regions, the lesser Green's function is calculated as $G^{<}(\mathbf{r},\mathbf{r}',\mathcal{E}) = G^{\mathrm{R}}(\mathbf{r},\mathbf{r}',\mathcal{E}) f_{\mathrm{G,B}}(\mathcal{E})$. The lesser Green's function in the dielectric is determined by $G^{<}(\mathbf{r},\mathbf{r}',\mathcal{E}) = G^{\mathrm{R}}(\mathbf{r},\mathbf{r}',\mathcal{E})\Sigma^{<}(\mathbf{r},\mathbf{r}',\mathcal{E})G^{\mathrm{A}}(\mathbf{r},\mathbf{r}',\mathcal{E})$. The lesser self energy of the left and right contact is given as $\Sigma^{<}_{\mathrm{G,B}}(\mathcal{E}) = \mathrm{i}\Im\left\{\Sigma^{\mathrm{R}}_{\mathrm{G,B}}(\mathcal{E})\right\} f_{\mathrm{G,B}}(\mathcal{E})$. The electron density and

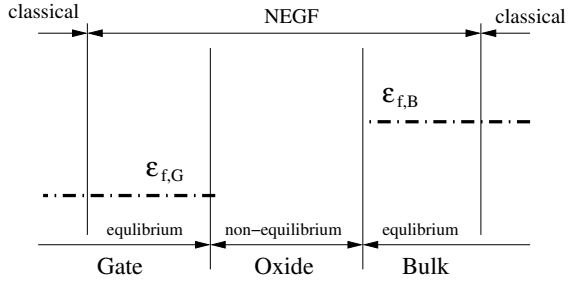

Fig. 1: The simulation domain is split into a classical lead region and a quantum mechanical device region. The gate and bulk contacts are assumed to be in thermal equilibrium.

978-1-4244-1753-7/08/$25.00 ©2008 IEEE

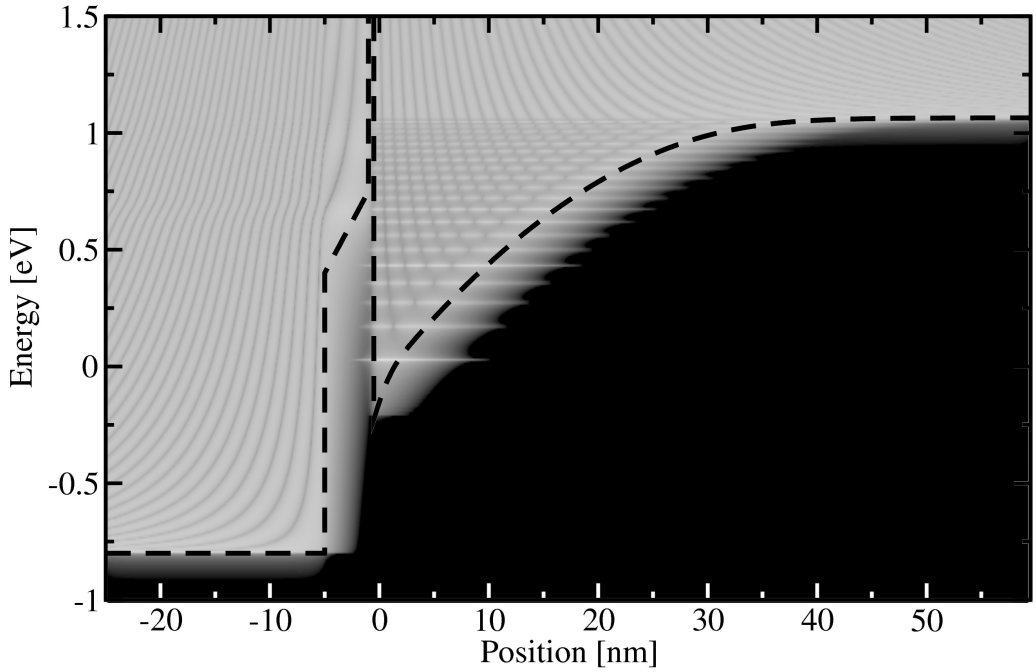

Fig. 2: Self-consistent band edge and the local density of states. Quantum mechanical effects like the penetration of the wavefunctions into classically forbidden regions and reflections at the barrier are clearly seen. Furthermore, in the channel the formation of quasi-bound states and the transition to the continuum states is observed.

the leakage current are given by the integrals

$$n(\mathbf{r}) = -2\mathrm{i} \int G^{<}(\mathbf{r},\mathbf{r},\mathcal{E}) \frac{\mathrm{d}\mathcal{E}}{2\pi} \,, \tag{5}$$

$$j(\mathbf{r}) = -\frac{\hbar q}{m^*} \int \left[(\nabla - \nabla') G^{<}(\mathbf{r},\mathbf{r}',\mathcal{E}) \right]\Big|_{\mathbf{r}'=\mathbf{r}} \frac{\mathrm{d}\mathcal{E}}{2\pi} \,. \tag{6}$$

III. Numerical Methods

In inversion, numerous quasi-bound states arise in the channel of a MOS transistor as displayed in Fig. 2. These states correspond to narrow resonances in the energy spectrum. To correctly calculate the integrals (5) and (6) these resonances need to be accurately resolved. Using a fixed, equidistant energy grid does not necessarily yield higher numerical accuracy but greatly increases the computational cost, since the Green's functions need to be solved for every energy grid point. Therefore, an adaptive energy integration method has been implemented [8]. One of the realized algorithms, which is based on the doubly adaptive quadrature routine reported in [9], is depicted in Fig. 3. The method utilizes Newton-Cotes quadrature of the order five, nine, 17 and 33.

Starting from an initial grid, for example, provided by a resonance finder to further increase numerical accuracy, the Green's functions are calculated for the given energies. Then the integral and the error are computed for all subintervals. The interval with the biggest contribution to the aggregated global error is then extracted from the datastructure and subdivided. If the integration error is reduced hereby, the two new subintervals are reinserted into the datastructure. Otherwise, the Green's functions on additional energy grid points are calculated and the next higher order Newton-Cotes rule is applied to the processed interval. This procedure is repeated until the previously chosen global error criterion is fulfilled. By this means, the algorithm generates an energy grid, automatically refined in critical ranges of the energy spectrum, namely near the potential of the contact regions and at the energies of the resonant states.

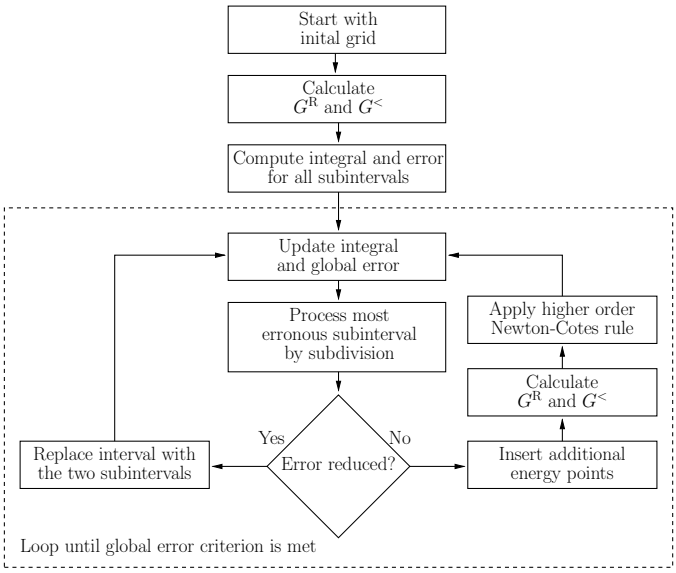

Fig. 3: Illustration of the doubly adaptive global quadrature routine.

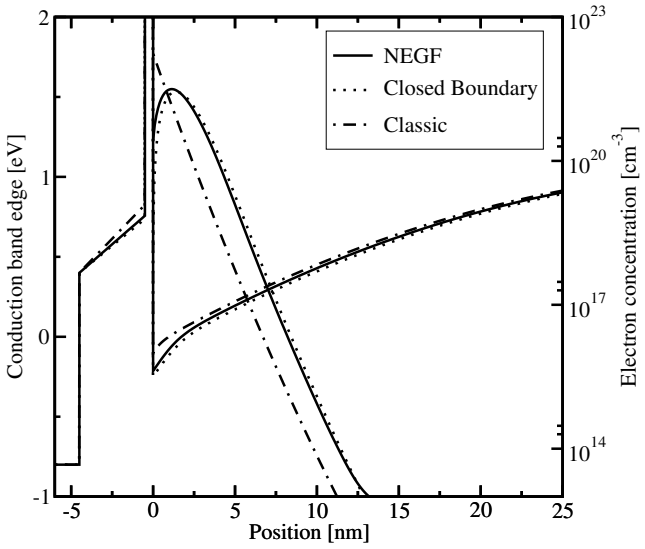

Fig. 4: Self-consistent bandedge and carrier concentration. While the classical carrier concentration reaches its maximum at the oxide interface, it is zero for the closed boundary model. For NEGF, penetration into the oxide occurs.

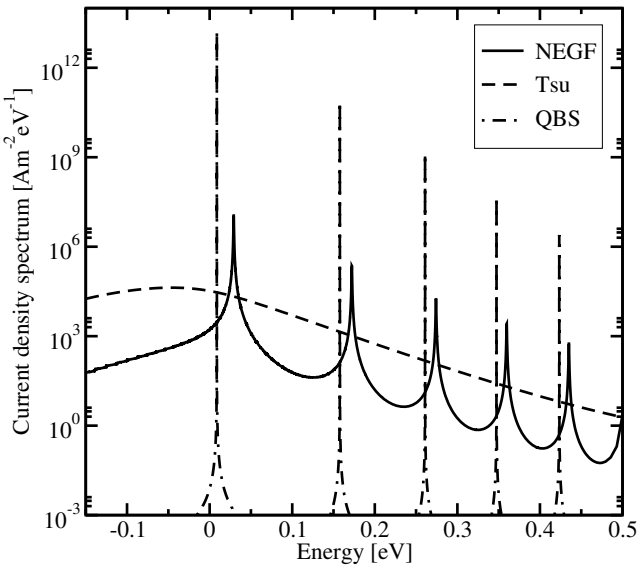

Fig. 5: Current spectrum displayed for Tsu Esaki, QBS and NEGF. Contrary to the QBS, the resonant peaks obtained by the Green's functions simulation show an energy broadening.

	QBS			NEGF	
	$\mathcal{E}_i$[meV]	τ_i[s]	I[Am^{-2}]	$\mathcal{E}_i$[meV]	I[Am^{-2}]
1	8.7	1.78×10^{-6}	10040.0	29.1	9477.4
2	157.7	2.37×10^{-7}	314.1	172.2	209.65
3	260.9	5.01×10^{-8}	27.45	274.0	17.15
4	347.4	1.17×10^{-8}	4.13	359.7	2.48
5	423.4	2.78×10^{-9}	0.92	435.0	0.54

Table 1: Overview of the first five quasi bound states and their contributions to the total current density. Due to the variation in the bandedge obtained through the self-consistent consideration of the charge in the channel, the resonant peaks given by NEGF are shifted to higher energies.

As opposed to previous works [10], the described method allows the NEGF formalism to be applied self-consistently with the electrostatic potential for the whole energy range and therefore, capture the influence of both the quasi-bound and the continuum states (cf. Fig 4).

IV. Results

For a gate stack in strong inversion, the current spectra of the Tsu-Esaki, the QBS-tunneling model and the NEGF formalism are shown in Fig. 5. The NEGF approach clearly shows the distinct resonant states. Compared to the QBS model, the peaks show a realistic broadening due to the scattering processes modeled by the optical potential. On the other hand, the resonances are completely neglected by the Tsu-Esaki model. This indicates that the QBS and the Tsu-Esaki models capture only the extreme cases of a quantized system and a free electron gas, respectively. For accumulation, the situation is shown in Fig. 6 and Fig. 7.

The capacitance-voltage characteristics is given in Fig. 8. For inversion, the closed boundary models predict a reduced capacitance because the wave function is set to zero at the interface to the oxide and omit the penetration into the dielectric. This effect shifts the charge centroid closer to the interface and increases the capacitance which is taken into account in the NEGF model. Surprisingly, all three models give a similar macroscopic leakage current as shown in Fig. 9 and confirmed by the data given in Table 1. However, there is a major difference in the current spectrum as shown Fig. 5.

V. Conclusion

We have implemented a full self-consistent approach to model the leakage current in high-k gate stacks. A discrepancy with respect to simpler models in the current spectrum has been observed. Therefore, any model sensitive to the changes in the current spectrum are affected by these effects. This is especially true for trap assisted tunneling models which are needed for the characterization of high-k materials.

Acknowledgment

This work has been supported by the Austrian Science Fund, special research program IR-ON (F2509).

References

[1] K. Mistry *et al.*, *Electron Devices Meeting, 2007. IEDM 2007. IEEE International* (2007), pp. 247–250.
[2] R. Tsu *et al.*, Appl. Phys. Lett. **22**, 562 (1973).
[3] R. Clerc *et al.*, J. Appl. Phys. **91**, 1400 (2002).
[4] R. C. Bowen *et al.*, J. Appl. Phys. **81**, 3207 (1997).
[5] M. Karner *et al.*, *Semiconductor Device Research Symposium, 2007 International* (2007), pp. 1–2.
[6] R. Lake *et al.*, physica status solidi (b) **204**, 354 (1997).
[7] A. Svizhenko *et al.*, J. Appl. Phys. **91**, 2343 (2002).
[8] O. Baumgartner *et al.*, *Technical Proceedings of the 2007 NSTI Nanotechnology Conference* (2007), Vol. 3, pp. 145–148.
[9] T. Espelid, BIT Numerical Mathematics **43**, 319 (2003).
[10] R. C. Bowen *et al.*, *Electron Devices Meeting, 1997. Technical Digest., International* (1997), pp. 869–872.

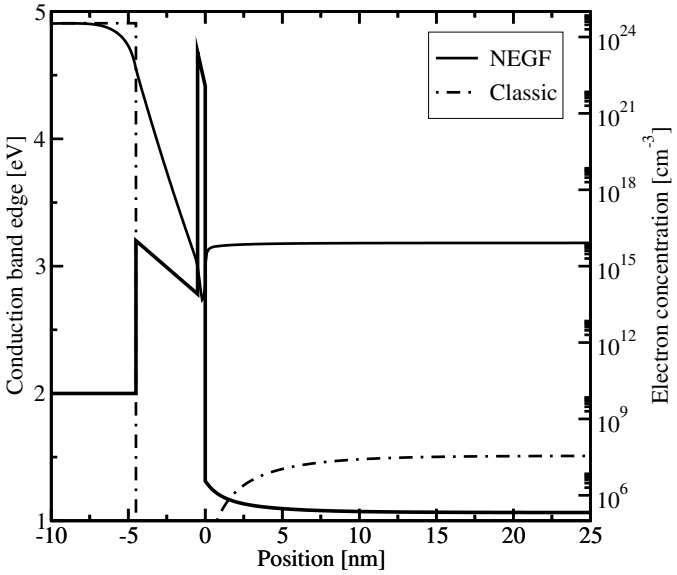

Fig. 6: Self-consistent band edge and electron concentration in accumulation. For NEGF, penetration into the oxide occurs.

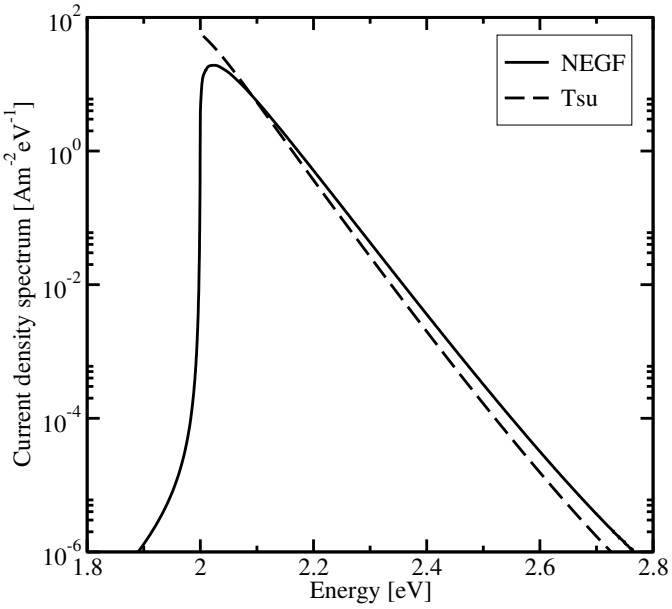

Fig. 7: Current spectrum for Tsu Esaki, QBS and NEGF. Contrary to the QBS, the resonant peaks obtained by the Green's functions simulation show an energy broadening.

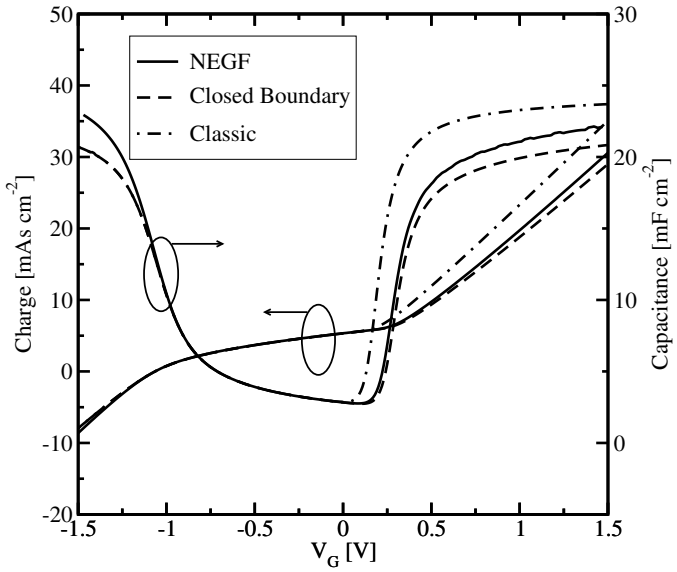

Fig. 8: The capacitance-voltage characteristics calculated using the semiclassical, the closed boundary, and the NEGF model.

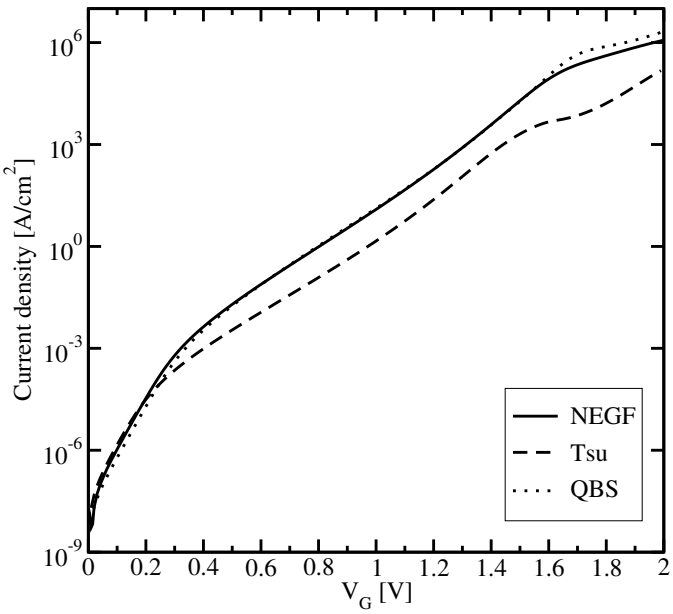

Fig. 9: The current-voltage characteristics show only a slight variation for the three different modeling approaches.